LETTER

doi:10.1038/nature10782

Single-molecule imaging of DNA pairing by RecA reveals a three-dimensional homology search

Anthony L. Forget[1,2] & Stephen C. Kowalczykowski[1,2]

DNA breaks can be repaired with high fidelity by homologous recombination. A ubiquitous protein that is essential for this DNA template-directed repair is RecA[1]. After resection of broken DNA to produce single-stranded DNA (ssDNA), RecA assembles on this ssDNA into a filament with the unique capacity to search and find DNA sequences in double-stranded DNA (dsDNA) that are homologous to the ssDNA. This homology search is vital to recombinational DNA repair, and results in homologous pairing and exchange of DNA strands. Homologous pairing involves DNA sequence-specific target location by the RecA–ssDNA complex. Despite decades of study, the mechanism of this enigmatic search process remains unknown. RecA is a DNA-dependent ATPase, but ATP hydrolysis is not required for DNA pairing and strand exchange[2,3], eliminating active search processes. Using dual optical trapping to manipulate DNA, and single-molecule fluorescence microscopy to image DNA pairing, we demonstrate that both the three-dimensional conformational state of the dsDNA target and the length of the homologous RecA–ssDNA filament have important roles in the homology search. We discovered that as the end-to-end distance of the target dsDNA molecule is increased, constraining the available three-dimensional (3D) conformations of the molecule, the rate of homologous pairing decreases. Conversely, when the length of the ssDNA in the nucleoprotein filament is increased, homology is found faster. We propose a model for the DNA homology search process termed 'intersegmental contact sampling', in which the intrinsic multivalent nature of the RecA nucleoprotein filament is used to search DNA sequence space within 3D domains of DNA, exploiting multiple weak contacts to rapidly search for homology. Our findings highlight the importance of the 3D conformational dynamics of DNA, reveal a previously unknown facet of the homology search, and provide insight into the mechanism of DNA target location by this member of a universal family of proteins.

The mechanism by which the RecA family of DNA strand exchange proteins (which include T4 UvsX, archaeal RadA and eukaryotic Rad51) locate DNA sequence identity is unknown. Ensemble studies have constrained possible mechanisms by establishing that ATP hydrolysis is not needed[3,4] and 1D sliding is not operative[5]. Consequently, the manner by which the RecA nucleoprotein filament promotes the efficient, rapid and accurate search for homology has remained undefined for decades[6]. Single-molecule methods have the potential to provide new insight into this long-standing question. In fact, magnetic tweezer experiments showed that the endpoint of homologous pairing can be detected as a change in the length of a single dsDNA target molecule[7,8]. However, the mechanism by which homology was found and DNA pairing occurred was not shown. Therefore, we sought to directly observe the manner by which RecA nucleoprotein filaments locate their homologous target in dsDNA.

Initially we attempted to directly observe fluorescent RecA nucleoprotein filaments interacting with bacteriophage λ dsDNA in real time by using total internal reflected fluorescence microscopy (TIRFM)[9]. Fully homologous fluorescent ssDNA that was complementary to three different loci of λ DNA (Fig. 1A) was generated by incorporation of 5-(3-aminoallyl) dUTP into ssDNA using polymerase chain reaction (PCR), followed with covalent attachment of ATTO565 (Supplementary Methods). RecA nucleoprotein filaments were assembled on these fluorescent ssDNA substrates in ensemble reactions containing ssDNA-binding protein (SSB) and the non-hydrolysable ATP analogue, ATPγS (5′-O-3′-thiotriphosphate)[4]. ATPγS was used to maintain the filament in its active form, eliminate filament disassembly and prevent dissociation of DNA pairing products[7,10–12]. Using

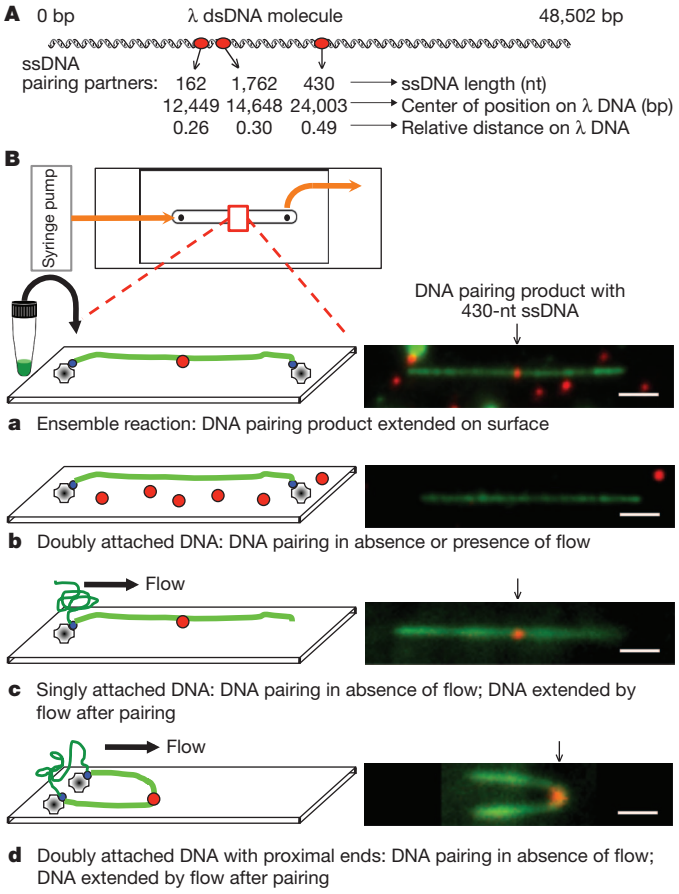

Figure 1 | DNA pairing by RecA, imaged using single-molecule TIRFM, indicates that the three-dimensional conformation of target dsDNA is important in the homology search. **A**, DNA substrates. **B**, DNA pairing between λ DNA (green) and RecA filament assembled on 430-nucleotide (nt) ssDNA (red). The ensemble reaction was examined by TIRFM (**B**, **a**). In *in situ* reactions dsDNA was attached before pairing; doubly attached extended DNA (**B**, **b**), singly attached DNA (**B**, **c**) and doubly attached DNA with ends in proximity (**B**, **d**). Homologously paired products were observed in **B**, **c** and **B**, **d** when DNA was relaxed by stopping flow and then extended by flow for visualization. Scale bars, 2.4 μm.

[1]Department of Microbiology, University of California, Davis, California 95616-8665, USA. [2]Department of Molecular and Cellular Biology, University of California, Davis, California 95616-8665, USA.

biochemical assays, we confirmed that the fluorescent ssDNA that was generated by this procedure was functional for RecA-mediated DNA pairing (Supplementary Fig. 1). The λ dsDNA, biotinylated at each end, was attached under flow to the interior surface of a single-channel microfluidic device (flowcell) (Fig. 1B). Owing to sequential attachment of each end to the streptavidin-coated surface, most DNA molecules were extended to nearly (~80%) B-form length, and extension could be maintained in the absence of flow (Fig. 1B, a, b).

To confirm DNA pairing at the homologous λ DNA target site, reactions were conducted under ensemble conditions, and products were extended on the surface of a flowcell for analysis by single-molecule, two-colour TIRFM; dsDNA was imaged by YOYO1 binding (green) and ssDNA by ATTO565 (red). DNA pairing products were observed; the sites of interaction coincided with the region of homology within the λ DNA molecule (Fig. 1B, a). For the 430-nucleotide ssDNA, all bound fluorescent ssDNA RecA filaments were at the homologous locus (observed fractional distance 0.51 ± 0.02; $n = 21$; Supplementary Fig. 2).

Next, we attempted to detect homologous pairing in real time using single-molecule TIRFM. Preformed RecA nucleoprotein filaments were introduced into a flowcell to which λ DNA molecules were tethered, buffer flow was stopped, and the reaction was monitored in real time (Fig. 1B, b). Although the dsDNA was readily visible, we failed to observe any interaction between the fluorescent nucleoprotein filaments and extended λ DNA, even for reaction periods longer than 1 h. However, we noticed that in addition to the desired doubly tethered extended λ DNA molecules, some DNA molecules were attached only by one end (Fig. 1B, c). When flow was stopped to score pairing with the doubly tethered λ DNA molecules, these singly tethered molecules relaxed to a randomly coiled state. Unexpectedly, when these unconstrained DNA molecules were subsequently re-extended by buffer flow, 80% ($n = 20$) revealed a stable pairing product (Fig. 1B, c). This finding suggested that either a free DNA end or a random coiled DNA was needed for pairing. In the same field of view, there were also λ DNA molecules that had both ends attached, but at a relatively close end-to-end distance (Fig. 1B, d). When the flow was stopped, we observed that these molecules also participated in homologous pairing during the time that flow was off, demonstrating that a free DNA end was not required. These unanticipated results revealed that DNA pairing did not occur on DNA that was extended to near its entropic elastic limit, and suggested that the DNA homology search required the 3D states that are accessible in randomly coiled DNA. Collectively, they suggested that a coiled conformation of the target dsDNA is crucial.

To address this possibility, we developed an alternative single-molecule imaging strategy that permitted reproducible measurement of the effects of dsDNA conformational structure, unperturbed by flow, on the DNA homology search process. This method uses a specialized flowcell (Fig. 2A), two optical laser traps operated in position-clamp mode, epifluorescent detection, fluorescent RecA–ssDNA filaments and a λ DNA dumbbell (a single λ DNA molecule with a 1-μm polystyrene bead attached at each end[13] (Supplementary Methods)). The DNA pairing assay was performed *in situ* using the dsDNA dumbbell target, and the dual optical trap configuration was used to reliably vary the end-to-end distance of the dsDNA. The flowcell has four channels and a flow-free reservoir. Movement of DNA dumbbells between channels of the flowcell was accomplished through stage translation, and manipulation of optical traps relative to one another was accomplished using a steering mirror controlling one of the traps. Each experiment (Fig. 2B and Supplementary Movie 1) consisted of six steps: first, in channel one, a streptavidin-coated bead was trapped in each of the two optical traps (Fig. 2B, a); second, the beads were moved to channel two to capture a λ dsDNA molecule (biotinylated on both ends and stained with YOYO1) on one bead (Fig. 2B, b); third, the beads were moved into channel three, and by independent steering of a trap, the distal end of the DNA was attached

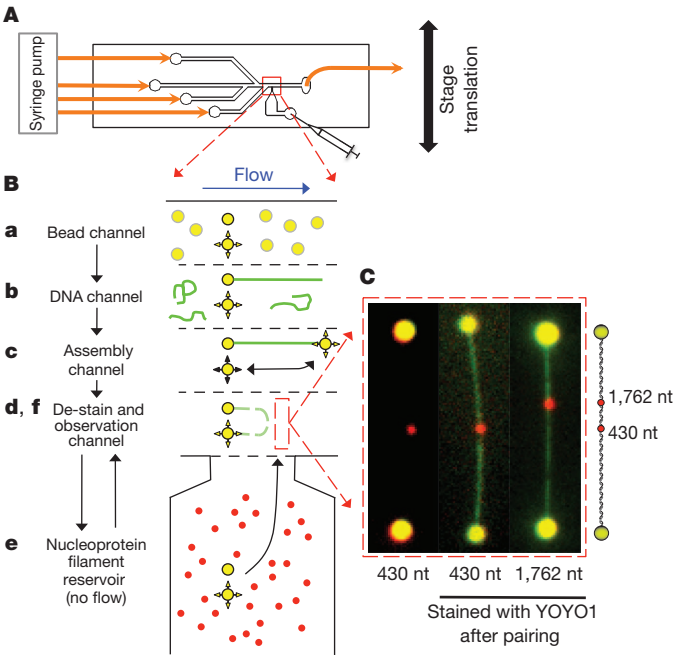

Figure 2 | Visualization of RecA-promoted DNA pairing with an individual optically trapped DNA dumbbell, imaged by epifluorescence. **A**, Four-channel flowcell with a flow-free reservoir. **B**, DNA dumbbell assembly and RecA-pairing reaction: two beads (yellow) are trapped (**B**, **a**); a λ DNA molecule (green) is captured on one bead (**B**, **b**); the free DNA end is captured with the second bead using a steerable optical trap (**B**, **c**); the centre-to-centre bead distance is set and YOYO1 is removed (**B**, **d**, de-stain); the DNA dumbbell is incubated in reservoir with RecA nucleoprotein filaments (red) (**B**, **e**) and DNA is extended to visualize products (**B**, **f**). **C,** Images of pairing products with 430- and 1,762-nucleotide nucleoprotein filaments.

to the second bead (Fig. 2B, c); fourth, the DNA-dumbbell was moved to the dye-free channel for de-staining, and the end-to-end distance was fixed (Fig. 2B, d); fifth, the DNA-dumbbell was moved to the flow-free reservoir containing the fluorescent ssDNA-RecA filaments (Fig. 2B, e); and sixth, after a defined incubation time, the DNA dumbbell was moved back to channel four, which is free of nucleoprotein filaments, extended to its contour length (~16 μm) and examined for DNA pairing products (Fig. 2B, f).

Shown in Fig. 2C are representative products of reactions in which the DNA dumbbells were initially held at a centre-to-centre bead distance of 2 μm and incubated for 2 min in the reservoir that contained RecA nucleoprotein filaments. For the two homologous ssDNA nucleoprotein filaments shown (430 nucleotides and 1,762 nucleotides), the pairing is clearly at the homologous locus. For a 2 min incubation with dsDNA at a bead-to-bead distance of 2 μm and the 430-nucleotide substrate, 90% of the dsDNA molecules ($n = 29$) contained a nucleoprotein filament stably bound to the expected region of homology (Fig. 3a). To determine the effect of end-to-end distance (that is, 3D conformation) on the RecA-mediated DNA pairing reaction, the reactions were performed at increasing bead separations (Fig. 3a). As the bead distance was increased from 2 μm to 8 μm, the efficiency of DNA pairing decreased to near zero, extrapolating to zero at ~9 μm; for comparison, in the TIRFM experiments in which no DNA pairing was detected *in situ*, the DNA end-to-end distance was ~13 μm.

We compared the time course of homologous pairing for fixed centre-to-centre bead distances of 2 μm and 6 μm (Fig. 3b) to determine the effect of decreasing DNA conformational states on the rate of the reaction. For the 2 μm separation, the rate of DNA pairing increased with a half-time of ~30 s and approached a yield of 100%. When the separation was increased to 6 μm, the rate slowed fourfold to a half-time of ~125 s, but nevertheless approached a yield of 100%

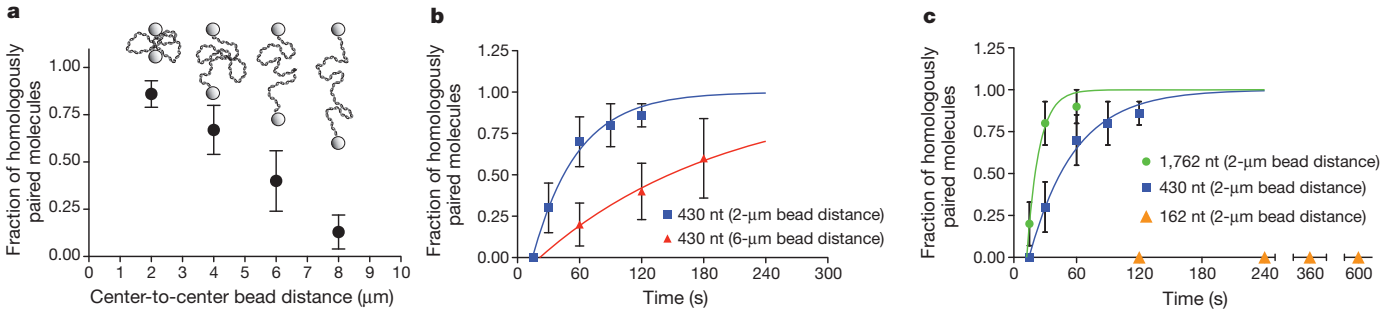

Figure 3 | DNA three-dimensional conformation and nucleoprotein filament length contribute to the homology search. **a**, Effect of DNA end-to-end distance; 430-nucleotide substrate (2 min). Error bars, s.e.m. from multiple experiments ($n = 10$ to 29). **b**, Time course; 430-nucleotide substrate: 2-μm (squares) and 6-μm (triangles) bead separation; respective pairing rates, 0.023 ($\pm$ 0.002) s^{-1} ($n \geq 10$) and 0.0056 ($\pm$ 0.0006) s^{-1} ($n \geq 5$). **c**, Effect of ssDNA length; 162 nucleotides (triangles; $n = 5$, 6, 4 and 2 at the times indicated), 430 nucleotides (squares; same data as Fig. 3b; $n \geq 10$) and 1,762 nucleotides (circles; $n \geq 10$); error bars, s.e.m.; 2-μm separation; respective rates: zero, 0.023 ($\pm$ 0.002) s^{-1}, and 0.086 ($\pm$ 0.026) s^{-1}.

(Fig. 3b). To establish the kinetic reaction order, we conducted single-molecule DNA pairing assays as a function of RecA nucleoprotein filament concentration (Supplementary Fig. 3). The reaction rate was independent of nucleoprotein filament concentration, showing that DNA pairing under these conditions is not diffusion limited, but that it is limited instead by a rate-determining unimolecular step as in the ensemble studies[14]. However, the pairing rate was dependent on dsDNA conformation and therefore was not dependent on the sequence recognition step itself.

To understand the nature of the complex that limits the rate of DNA pairing, we varied the length of RecA nucleoprotein filaments. Shown in Fig. 3c is a comparison of the time courses for 162-, 430- and 1,762-nucleotide nucleoprotein filaments. Increasing the ssDNA length approximately fourfold, from 430 to 1,762 nucleotides, increased the observed rate of pairing approximately 3.8-fold. However, when the length of the ssDNA was decreased to 162 nucleotides, we did not observe any stably bound homologously paired products after incubations for 10 min at the closest bead-to-bead distance possible (2 μm), despite this substrate being active in ensemble DNA pairing reactions (Supplementary Fig. 2). We conclude that the length of the RecA nucleoprotein filament is a crucial factor in the rate-limiting step of homologous pairing.

In addition to the anticipated stable, homologously paired end products, short-lived non-homologous interactions were observed (Fig. 4a). These events, which occurred outside of the homologous regions, were relatively unstable and dissociated during the movement of the molecule from the reservoir to the observation channel, during the separation of beads or after the λ DNA molecule was extended (Supplementary Movie 2). These heterologous events lasted no more than a few tens of seconds and never persisted on a timescale of minutes. When the molecules from the 2-μm data set were analysed, 22% of the reactions with the 430-nucleotide ssDNA and 40% of reactions with the 1,762-nucleotide ssDNA had these unstable heterologously paired intermediates (Fig. 4b), and for the 162-nucleotide ssDNA, only 1 heterologously bound filament was seen out of 28 molecules.

Some intermediates of the pairing process had a second filament bound non-specifically to spatially separated regions of the λ DNA molecule. For such a heterologously bound nucleoprotein filament, when the relaxed DNA molecule was moved into the observation channel and the beads were separated for observation, the existence of a loop could be inferred from a sudden recoil of the homologously paired spot. As the beads were separated, the weaker of the two heterologous interactions was released, and there was a simultaneous movement ('jump') of the fluorescence at the homologous pairing locus (Fig. 4a and Supplementary Movie 3) resulting from the release of DNA that was constrained in the loop. Approximately 12% ($n = 50$) of the DNA dumbbells showed loop release events for the 430-nucleotide nucleoprotein filament and, consistent with expectations, when the length of the nucleoprotein filament was increased to 1,762 nucleotides, the number of molecules with transient loop structures increased to 47% ($n = 30$) (Fig. 4c).

Our results clearly establish that both the 3D conformation of dsDNA and the length of the nucleoprotein filament are important determinants of the rate for DNA homologous pairing. These findings lead us to propose a model termed 'intersegmental contact sampling' to describe the search for homology by a RecA nucleoprotein filament (Fig. 4d). One of the key features of the model is that the RecA nucleoprotein filament has a polyvalent interaction surface that is capable of binding simultaneously and non-specifically, but weakly, with non-contiguous segments of dsDNA. The second related feature of this

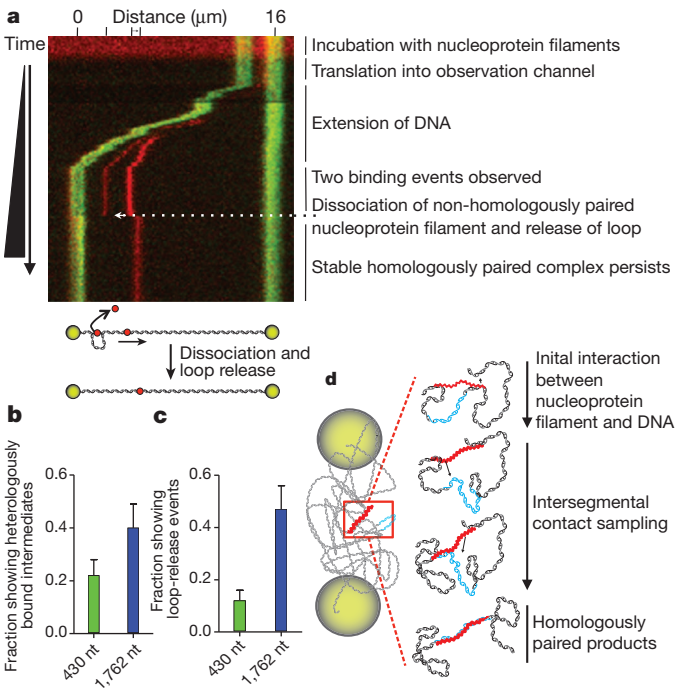

Figure 4 | RecA nucleoprotein filaments exhibit transient non-homologous interactions and loop-release events. **a**, Kymograph of DNA dumbbell during bead separation (Fig. 2B, f). Distance scale (top) and tick marks show positions of beads (green) and nucleoprotein filaments (red); illustration depicts dissociation of heterologously bound filament. **b**, **c**, Fraction of dsDNA dumbbells with non-homologously bound intermediates (**b**) and loop release events (**c**); 430-nucleotide (blue) and 1,762-nucleotide (green) filaments; $n = 50$ and 30, respectively. Error bars, s.e.m. **d**, Model for RecA homology search by intersegmental contact sampling; for simplicity, only two simultaneous points of interaction are depicted.

model is that 3D conformational entropy of the dsDNA greatly enhances the probability that DNA sequence homology will be found through iterated homology sampling, using multiple weak contacts, by this polyvalent filament. This model is compatible both with our key experimental findings, which we expect would apply to the search in the presence of ATP as well, and with the involvement of heterologously bound intermediates that have been inferred from biochemical studies[15,16]. Our data show that dsDNA extended to near contour length fails to produce homologously paired products. This observation provides an explanation for the observation that the formation of stable DNA pairing products in single-molecule studies using magnetic tweezers required negative plectonemic supercoils in the DNA target[7,8]. By contrast, when a ssDNA–RecA filament was extended to near its contour length, homologous pairing with fully homologous coiled dsDNA occurred[7], which is compatible with our finding that the coiled structure of dsDNA is essential to the homology search. Here we established that as the end-to-end distance of the dsDNA was decreased, allowing it to assume a more random coil-like 3D conformation, the rate of DNA pairing increased because the local DNA concentration increases, and the likelihood that DNA segments will be in close proximity also greatly increases. The increased local DNA concentration results in a greater statistical probability that a single nucleoprotein filament can simultaneously interact with and sample multiple regions of the same DNA molecule. This, in turn, is manifest as a kinetically more efficient homology sampling process. In further support of the intersegmental contact sampling model, when the length of the ssDNA in the nucleoprotein filament is increased, the observed rate of pairing, as well as the number of nucleoprotein filaments with multiple, transient, heterologous intersegmental interactions is increased. This shows that longer nucleoprotein filaments can simultaneously and independently sample more segments of the target dsDNA than shorter nucleoprotein filaments. Kinetically, our findings are consistent with the following two-step scheme:

$$\mathrm{NPF} + \mathrm{dsDNA} \underset{}{\overset{K_{het}}{\rightleftharpoons}} \underset{\text{(heterologously bound)}}{\mathrm{NPF{-}dsDNA}} \overset{k_s}{\rightarrow} \underset{\text{(homologously paired)}}{\mathrm{NPF{-}dsDNA}}$$

where K_{het} is the equilibrium constant for the binding of a RecA nucleoprotein filament (NPF) to heterologous dsDNA (the kinetic steps comprising K_{het} are rapid compared to k_s) and k_s is the rate-limiting unimolecular rate constant for intersegmental homology searching step within the dsDNA molecule or domain. In general, this kinetic formalism predicts a hyperbolic dependence of homologous pairing on the component concentrations unless the equilibrium constant for formation of the heterologous complex is large; when this is case, the observed rate is defined by the first-order rate constant, k_s. Given that the rate of target location is independent of nucleoprotein filament concentration, this implies that the heterologously bound complex is saturated at a filament concentration of 100 pM (Supplementary Fig. 3), placing a limit on the apparent equilibrium dissociation constant of <10 pM (that is, $K_{het} > 10^{11}$ M^{-1}). In the context of this kinetic model, values for k_s are defined by the experiments in Fig. 3b, c, which show that the rate of the intersegmental homology search decreases fourfold when the DNA end-to-end distance increases from 1 μm to 5 μm and increases approximately fourfold when the ssDNA length increases approximately fourfold. The correlation of rate with the length of ssDNA suggests that the intradomainal search is enhanced proportionately by the increase in either heterologous contacts or the reach of the longer ssDNA. In many regards, the homology search by RecA has parallels to target location by sequence-specific DNA-binding proteins, with the notable exception that the specificity of the RecA filament is determined by the sequence of the associated ssDNA. Seminal work on the DNA target selection by transcriptional regulatory proteins identified sliding, hopping and intersegmental transfer as potentially facilitating mechanisms[17,18]. Here we have established intersegmental transfer as the operative pathway used by RecA to find DNA sequence homology; this behaviour is distinct from the sliding and hopping used to enhance the rate of target location by most regulatory proteins, which are typically univalent or bivalent with regard to site binding[18]. Our approach now provides a framework for future studies on the previously mysterious homology search by recombination proteins. It is applicable to studies of more complex systems such as eukaryotic Rad51, as it can provide insight into the function of the many accessory proteins that enhance DNA pairing[9]. Finally, the imaging strategy and flow-free cell design can easily be adapted to visualize target location and mechanism of processes as diverse as DNA replication and repair, RNA interference, transcription and protein translation, in which the 3D conformations of nucleic acids are undoubtedly important.

METHODS SUMMARY

RecA and SSB were purified as described[19,20]. Fluorescent ssDNA was prepared as detailed in the Supplementary Information. Nucleoprotein filaments were formed as described[4] in SM buffer (25 mM Tris acetate (Tris-OAc) (pH 7.5), 1 mM DTT and 4 mM $Mg(OAc)_2$), SSB (at a ratio of 1 SSB monomer to 11 nucleotides), 2 nM molecules fluorescent ssDNA, and 1 mM ATPγS were incubated for 10 min at 37 °C; RecA was added at 1 monomer per 1.7 nucleotides, and incubated 1 h. Nucleoprotein filaments were diluted to 0.2 nM before use.

For DNA pairing using TIRFM, biotinylated λ DNA (1 pM, molecules) in SM2 (SM with 50 mM NaCl) was bound to the flowcell and then washed to remove free DNA, and to attach the second DNA end. Reactions were started by addition of 0.2 nM nucleoprotein filaments. For ensemble experiments visualized by TIRFM, nucleoprotein filaments and λ DNA were incubated for 1 h (162-nucleotide substrate) or 30 min (430-nucleotide substrate) at 37 °C.

Visualization of RecA-mediated pairing with individual DNA dumbbells was performed at 37 °C. The flowcell was treated for 1 h with BSA (1 mg ml^{-1}) in SM3 (50 mM Tris-OAc (pH 8.2), 50 mM DTT, 1 mM $Mg(OAc)_2$ and 15% sucrose). Biotinylated λ DNA and buffers were pumped into the flowcell at a linear flow rate of ~100 μm s^{-1}. Channels contained SM3, 18 fM streptavidin-coated polystyrene beads (1 μm, Bangs Laboratories) and 5 nM YOYO-1 (Invitrogen) (Fig. 2B, a); SM3, 100 nM YOYO1 and 10 pM (molecules) biotinylated λ DNA (Fig. 2B, b); SM3 (Fig. 2B, c); SM and 15% sucrose (Fig. 2B, d, f). The reaction reservoir contained 0.2 nM nucleoprotein filaments in SM with 15% sucrose and 0.5 mM ATPγS (Fig. 2B, e).

Full Methods and any associated references are available in the online version of the paper at www.nature.com/nature.

Received 12 September; accepted 12 December 2011.
Published online 8 February 2012.

1. Kowalczykowski, S. C., Dixon, D. A., Eggleston, A. K., Lauder, S. D. & Rehrauer, W. M. Biochemistry of homologous recombination in *Escherichia coli*. *Microbiol. Rev.* **58,** 401–465 (1994).
2. Menetski, J. P. & Kowalczykowski, S. C. Interaction of recA protein with single-stranded DNA. Quantitative aspects of binding affinity modulation by nucleotide cofactors. *J. Mol. Biol.* **181,** 281–295 (1985).
3. Kowalczykowski, S. C. & Krupp, R. A. DNA-strand exchange promoted by RecA protein in the absence of ATP: implications for the mechanism of energy transduction in protein-promoted nucleic acid transactions. *Proc. Natl Acad. Sci. USA* **92,** 3478–3482 (1995).
4. Menetski, J. P., Bear, D. G. & Kowalczykowski, S. C. Stable DNA heteroduplex formation catalyzed by the *Escherichia coli* RecA protein in the absence of ATP hydrolysis. *Proc. Natl Acad. Sci. USA* **87,** 21–25 (1990).
5. Adzuma, K. No sliding during homology search by RecA protein. *J. Biol. Chem.* **273,** 31565–31573 (1998).
6. Kowalczykowski, S. C. Biochemistry of genetic recombination: energetics and mechanism of DNA strand exchange. *Annu. Rev. Biophys. Biophys. Chem.* **20,** 539–575 (1991).
7. Fulconis, R., Miné, J., Bancaud, A., Dutreix, M. & Viovy, J. L. Mechanism of RecA-mediated homologous recombination revisited by single molecule nanomanipulation. *EMBO J.* **25,** 4293–4304 (2006).
8. van der Heijden, T. *et al.* Homologous recombination in real time: DNA strand exchange by RecA. *Mol. Cell* **30,** 530–538 (2008).
9. Forget, A. L. & Kowalczykowski, S. C. Single-molecule imaging brings Rad51 nucleoprotein filaments into focus. *Trends Cell Biol.* **20,** 269–276 (2010).
10. McEntee, K., Weinstock, G. M. & Lehman, I. R. Binding of the recA protein of *Escherichia coli* to single- and double-stranded DNA. *J. Biol. Chem.* **256,** 8835–8844 (1981).
11. Honigberg, S. M., Gonda, D. K., Flory, J. & Radding, C. M. The pairing activity of stable nucleoprotein filaments made from recA protein, single-stranded DNA, and adenosine 5′-(gamma-thio)triphosphate. *J. Biol. Chem.* **260,** 11845–11851 (1985).

12. Galletto, R., Amitani, I., Baskin, R. J. & Kowalczykowski, S. C. Direct observation of individual RecA filaments assembling on single DNA molecules. *Nature* **443,** 875–878 (2006).
13. van Mameren, J. *et al.* Counting RAD51 proteins disassembling from nucleoprotein filaments under tension. *Nature* **457,** 745–748 (2009).
14. Julin, D. A., Riddles, P. W. & Lehman, I. R. On the mechanism of pairing of single- and double-stranded DNA molecules by the recA and single-stranded DNA-binding proteins of *Escherichia coli*. *J. Biol. Chem.* **261,** 1025–1030 (1986).
15. Gonda, D. K. & Radding, C. M. By searching processively recA protein pairs DNA molecules that share a limited stretch of homology. *Cell* **34,** 647–654 (1983).
16. Tsang, S. S., Chow, S. A. & Radding, C. M. Networks of DNA and recA protein are intermediates in homologous pairing. *Biochemistry* **24,** 3226–3232 (1985).
17. Berg, O. G., Winter, R. B. & von Hippel, P. H. Diffusion-driven mechanisms of protein translocation on nucleic acids. 1. Models and theory. *Biochemistry* **20,** 6929–6948 (1981).
18. Berg, O. G. in *The Biology of Nonspecific DNA Protein Interactions* (ed. Revzin, A.) 71–85 (CRC, 1990).
19. Mirshad, J. K. & Kowalczykowski, S. C. Biochemical characterization of a mutant RecA protein altered in DNA-binding loop 1. *Biochemistry* **42,** 5945–5954 (2003).
20. Harmon, F. G. & Kowalczykowski, S. C. RecQ helicase, in concert with RecA and SSB proteins, initiates and disrupts DNA recombination. *Genes Dev.* **12,** 1134–1144 (1998).

Supplementary Information is linked to the online version of the paper at www.nature.com/nature.

Acknowledgements We are grateful to members of the laboratory for their comments on this work. A.L.F. was funded by an American Cancer Society Postdoctoral Fellowship (PF-08–046–01-GMC) and S.C.K. was supported by the National Institutes of Health (GM-62653 and GM-64745).

Author Contributions A.L.F. and S.C.K. conceived the general ideas, designed the experiments and interpreted the data. A.L.F. performed experiments. A.L.F. and S.C.K. wrote the manuscript.

Author Information Reprints and permissions information is available at www.nature.com/reprints. The authors declare no competing financial interests. Readers are welcome to comment on the online version of this article at www.nature.com/nature. Correspondence and requests for materials should be addressed to S.C.K. (sckowalczykowski@ucdavis.edu).

METHODS

Microscope. The instrument that was developed was based on an Eclipse TE2000-U inverted microscope with a total internal reflected fluorescence (TIRF) attachment (Nikon) using a CFI Plan Apo TIRF 100×, 1.45 numerical aperture oil-immersed objective. Infrared laser trapping, operated in position-clamp mode, was achieved almost exactly as previously described[21] with the addition of a polarizer (Newport) to split the beam and generate two traps, and a steering mirror (Newport) to control the *x*–*y* position of one of the beams. Fluorescence of the sample in TIRF mode was achieved by excitation using a Cyan 488-nm laser (Picarro) or a 561-nm laser (Cobolt). Epifluorescence illumination was achieved with an X-Cite 120-W mercury vapour lamp (Lumen Dynamics). The fluorescence emission was directed through a polychroic mirror (centre wavelength 515 nm, bandwidth 30 nm; and centre wavelength 600, bandwidth 40 nm; Chroma). Light was guided into a Dual-View apparatus (Optical Insights) where the green and red components were spatially separated (dichroic 565dxcr, emission HQ515/30 nm and HQ600/40 nm, Chroma). Movies were captured on a DU-897E iXon CCD camera (Andor, 100-ms exposure) and processed using IQ imaging software (Andor).

Biotinylated λ duplex DNA. Multiple biotin moieties were incorporated into both ends of bacteriophage λ DNA (NEB) by an end-filling reaction. A 30-µl reaction contained 1× NEB buffer number 2, 33 µM each of dATP, dTTP, dCTP and biotin-11-dGTP (Perkin Elmer), 5 µg λ DNA and 5 units of Klenow exo$^-$ (NEB). The reaction was incubated for 15 min at 25 °C then terminated by the addition EDTA to a final concentration of 10 mM and heat inactivation of Klenow at 75 °C for 20 min. The reaction was then diluted to a 100-µl final volume with Nanopure water (Millipore) and passed through an S-400 spin column (GE Healthcare) equilibrated with TE buffer (10 mM Tris-HCl (pH 7.5) and 1 mM EDTA).

Fluorescent ssDNA substrates. DNA primer sequences that were used to amplify defined regions of λ DNA by PCR are the following, for: an 87-bp product for D-loop assay with pUC19 supercoiled DNA: forward primer 5′-biotin-CGACGGCCAGTGAATTCCCCGA-3′, reverse primer 5′-TTACGCCAAGCTTACTCGGGAAACAT-3′; a 162-bp product (identical to λ DNA between base pairs 12,368–12,529): forward primer 5′-biotin-TAACGTCATGTCAGAGCAGAAAAAG-3′, reverse primer 5′-GCAATACCATCAAAGGTCTGCGTG-3′; a 430-bp product (identical to λ DNA between base pairs 23,788–24,217): forward primer 5′-biotin-ACTGTTCTTGCGGTTTGGAGG-3′, reverse primer 5′-CTATCGGAAGTTCACCAGCCAG-3′; and a 1,762-bp product (identical to λ DNA between base pairs 13,767–15,528): forward primer 5′-biotin-GGATGCGGTGAACTTCGTCAAC-3′, reverse primer 5′-CCCCTTACTGCTTCCTTTACCC-3′.

PCR reactions contained 1× ThermoPol buffer (NEB), 0.2 mM dATP, 0.2 mM dCTP, 0.2 mM dGTP, 0.1 mM dTTP, 0.2 mM 5-(3-aminoallyl) dUTP (Fermentas), 0.25 ng µl^{-1} λ DNA (NEB) (pUC19 for a 87-nucleotide substrate), 0.5 µM each primer and 0.05 U µl^{-1} Vent exo$^-$ polymerase (NEB). The thermocycler (iCycler, Bio-Rad) program involved initial denaturation at 95 °C for 2 min, 30 cycles of a denaturation phase at 95 °C for 30 s, an annealing phase at 60.6, 63, 62.2 or 59.4 °C for 30 s, for 87-, 162-, 430- or 1762-nucleotide products, respectively, and an extension phase at 72 °C for 0.25, 0.25, 1 and 5 min for 87-, 162-, 430- and 1762-nucleotide products, respectively. The final PCR step was extension at 72 °C for 5 min. The reactions were then processed with a QIAquick PCR purification kit (Qiagen). Following purification, the DNA was ethanol-precipitated at −20 °C. To fluorescently label the PCR products, a 20-µl reaction containing 10–20 µg of PCR-generated DNA containing amine-modified nucleotides, 200 mM sodium bicarbonate (pH 9.0) and 5 mM ATTO565 NHS-ester (ATTO-TEC GmbH) was incubated for 1–2 h at 25 °C while protected from light. Alexa Fluor 488 succinimidyl ester (Invitrogen) was used to label the 87-nucleotide substrate used in the D-loop assay. Following incubation, 180 µl Nanopure water was added and a QIAquick PCR purification kit (Qiagen) was used to remove free label. Purified labelled DNA was stored at 4 °C until the strand-separation step. Alkali denaturation in combination with the single 5'-biotin incorporated from the forward primer in the PCR reaction was used to produce ssDNA from the fluorescently labelled duplex PCR product as follows: 800 µl avidin-agarose (400 µl settled gel; Thermo Scientific) was prepared in a 1.5-ml Eppendorf tube using centrifugation to pellet agarose. All centrifugation steps were performed using a bench-top centrifuge at 4,524*g* for 1 min. The resin was pelleted and washed three times with 1 ml binding and wash buffer (10 mM Tris-HCl (pH 7.5), 1 mM EDTA and 150 mM NaCl). Fluorescently labelled biotinylated dsDNA (~10–20 µg, from the PCR reaction above) was diluted to 1 ml with binding and wash buffer. The diluted DNA was added to the prepared avidin-agarose, and mixed end-over-end for 1 h while protected from light. The agarose and bound DNA were pelleted by centrifugation and washed three times with 1 ml binding and wash buffer to remove unbound DNA. The ssDNA was eluted by alkali denaturation of the dsDNA, by addition of 200 µl of 0.15 M NaOH to the pelleted agarose and mixing end-over-end for 10 min to release the non-biotinylated strand. The slurry was transferred to an empty micro-spin column (Bio-Rad) and centrifuged at 4,700*g* to recover the eluted ssDNA. A Microspin S-400 column (GE Healthcare) was used to exchange the ssDNA into the TE buffer. Samples of each fraction were analysed by polyacrylamide or agarose gel electrophoresis. Fractions containing ssDNA were pooled, purified and concentrated with QIAquick PCR purification kit (Qiagen). The DNA concentration was determined using an extinction coefficient of 8,919 M^{-1} cm^{-1} at 260 nm, taking into account a correction factor of 0.34 for absorbance at 260 nm by the dye. The dye concentration was determined using an extinction coefficient of 120,000 M^{-1} cm^{-1} at 563 nm.

Flowcell fabrication. Channels and holes were etched by CO_2 laser into glass slides (Fisher Scientific 25 × 75 × 1 mm) covered with an adhesive abrasive blasting mask (Epilog) using a 30 W Mini-24 Laser Engraver (Epilog Lasers). Following the engraving step, the slides were blasted using 220 grit silicon carbide (Electro Abrasives) to remove residual laser-ablated glass from the channels. A cover glass (Corning No. 1, 24 × 60 mm) was attached with ultraviolet Optical adhesive number 74 (Norland Products) applied through capillary action. The adhesive was cured by placing the flowcell 30 cm from a 100 W HBO lamp (Zeiss) for 20 min followed by a final heat curing at 70 °C for 12 h. PEEK tubing with 0.5 mm inner diameter (Upchurch Scientific) was inserted into each of the etched holes to create inlet and outlet connection ports using 5 min Epoxy (Devcon).

Surface preparation of single-channel flowcell for TIRFM experiments. The surface modification procedure was done at 25 °C. The flowcells were cleaned with 1 M NaOH for 30–60 min, and washed twice with 1 ml Nanopure water and then with 1 ml of buffer (25 mM Tris-OAc (pH 7.5), 50 mM NaCl). 1 mg ml^{-1} biotinylated BSA (Thermo Scientific) in the above buffer was then incubated in the flowcell for 5 min and then washed with 1 ml of buffer. After this, 0.1 mg ml^{-1} streptavidin (Promega) in buffer was incubated in the flowcell for 5 min then washed with 1 ml of buffer. Finally, the flowcell was blocked with 1.5 mg ml^{-1} Roche Blocking Reagent (Roche) in buffer for 30–60 min and washed with 1 ml buffer. The prepared flowcell was then mounted on the microscope and attached to the syringe pump (KD Scientific).

D-loop assay. RecA and SSB were purified as previously described[19,20]. The AlexaFluor 488-labelled 87-nucleotide ssDNA substrate was prepared as described above. A 10-µl reaction containing 25 mM Tris-HCl (pH 7.5), 10 mM $MgCl_2$, 1 mM DTT, 2 mM ATPγS, 100 µg ml^{-1} BSA, 4.5 µM RecA and 105 nM fluorescently labelled 87-nucleotide ssDNA was incubated for 8 min at 37 °C. The reaction was started with the addition of 35 nM supercoiled DNA (pUC19) and incubated at 37 °C for 20 min. The reaction was stopped by mixing with 5 µl of stop solution (4.8% SDS, 7 mg ml^{-1} proteinase K) and incubating for 10 min at 37 °C. Products were resolved by electrophoresis in a 1% ultrapure agarose gel (Invitrogen) using TAE (40 mM Tris, 20 mM acetic acid and 1 mM EDTA) at 100 V until the bromophenol blue had migrated 4 cm. The gel was imaged and analysed with a STORM scanner and Image Quant software (Molecular Dynamics). The efficiency of the reaction was calculated as the fraction of ssDNA that formed D-loops multiplied by three to correct for the threefold molar excess of ssDNA relative to supercoiled pUC19 in the reaction.

Single-molecule DNA pairing experiments. Nucleoprotein filaments were formed essentially as described previously[4] in SM buffer (25 mM Tris-OAc (pH 7.5), 1 mM DTT and 4 mM $Mg(OAc)_2$); SSB (at a ratio of 1 SSB monomer to 11 nucleotides), 2 nM molecules fluorescent ssDNA and 1 mM ATPγS were incubated for 10 min at 37 °C. RecA was added at a ratio of 1 monomer to 1.7 nucleotides and incubated for 1 h. Nucleoprotein filaments were then diluted tenfold to a final concentration of 0.2 nM in buffer before introduction into the flowcell. In the DNA pairing experiments using TIRFM, biotinylated λ DNA (1 pM, molecules) in SM2 buffer (SM and 50 mM NaCl) was introduced into the flowcell and allowed to bind for several minutes. The flowcell was then washed with 500 µl SM2 buffer to remove free DNA as well as to extend and attach the second end of the λ DNA molecules. The reaction was started by the addition of 0.2 nM nucleoprotein filaments in SM2 buffer. For ensemble experiments visualized by TIRFM, the nucleoprotein filaments and λ DNA were incubated for 1 h (162-nucleotide substrate) or 30 min (430 nucleotide substrate) at 37 °C before visualization in a single-channel flowcell.

Visualization of RecA-mediated pairing with individual DNA dumbbells was performed at 37 °C. The flowcell surface was treated for 1 h with BSA (1 mg ml^{-1}) in single-molecule (SM3) buffer (50 mM Tris-OAc (pH 8.2), 50 mM DTT, 1 mM $Mg(OAc)_2$ and 15% sucrose). Biotinylated λ DNA and buffers were pumped at a linear flow rate of ~100 µm s^{-1} into the flowcell. The channels contained SM3 buffer, 18 fM streptavidin-coated polystyrene beads (1 µm; Bangs Laboratories) and 5 nM YOYO-1 (Invitrogen) (Fig. 2B, a); SM3 buffer, 100 nM YOYO1, and 10 pM (molecules) biotinylated λ DNA (Fig. 2B, b); SM3 buffer (Fig. 2B, c); SM buffer and 15% sucrose (Fig. 2B, d, f). The reaction reservoir contained 0.2 nM nucleoprotein filaments in SM with 15% sucrose and 0.5 mM ATPγS (Fig. 2B, e).

Data analysis. Data were analysed using GraphPad Prism v5.04. The kinetic data were fit to a single exponential function ($Y = Y_0 + (\text{Plateau} - Y_0)(1 - e^{-kx})$). In Fig. 4b, c, the time courses do not pass through the origin. We are not certain whether this is an intrinsic characteristic of the homology search or a limitation of the experimental procedure: for example, the time for the DNA to relax from flow-induced stretching after movement into the reservoir. We note that the half-time for the relaxation of extended λ DNA is ~6 s (ref. 22); during this time the dsDNA is not in its equilibrium coiled configuration and initial interaction with the RecA nucleoprotein filament would be limited by the DNA polymer dynamics.

21. Bianco, P. R. *et al.* Processive translocation and DNA unwinding by individual RecBCD enzyme molecules. *Nature* **409,** 374–378 (2001).
22. Perkins, T. T., Quake, S. R., Smith, D. E. & Chu, S. Relaxation of a single DNA molecule observed by optical microscopy. *Science* **264,** 822–826 (1994).